Journal of Power Sources 254 (2014) 258–267

Contents lists available at ScienceDirect

Journal of Power Sources

journal homepage: www.elsevier.com/locate/jpowsour

Improved adaptive state-of-charge estimation for batteries using a multi-model approach

Huazhen Fang [a], Xin Zhao [a], Yebin Wang [b,*], Zafer Sahinoglu [b], Toshihiro Wada [c], Satoshi Hara [c], Raymond A. de Callafon [a]

[a] Department of Mechanical & Aerospace Engineering, University of California, San Diego, CA 92093, USA
[b] Mitsubishi Electric Research Laboratories, 201 Broadway, Cambridge, MA 02139, USA
[c] Advanced Technology R&D Center, Mitsubishi Electric Corporation, 8-1-1, Tsukaguchi-honmachi, Amagasaki City 661-8661, Japan

HIGHLIGHTS

- We propose to perform adaptive SoC estimation using multiple models.
- We build an SoC estimation algorithm via fusing estimates based on multiple models.
- The algorithm achieves effective SoC estimation against complicated battery dynamics.
- We validate the effectiveness of the algorithm via both simulation and experiments.
- The multi-model framework can be extended to other tasks for battery management.

ARTICLE INFO

Article history:
Received 4 October 2013
Received in revised form
21 November 2013
Accepted 2 December 2013
Available online 12 December 2013

Keywords:
State-of-charge
Adaptive estimation
Multiple models
State and parameter estimation
Nonlinear observability
Iterated extended Kalman filter

ABSTRACT

Adaptive estimation of the state-of-charge (SoC) for batteries is increasingly appealing, thanks to its ability to accommodate uncertain or time-varying model parameters. We propose to improve the adaptive SoC estimation using *multiple models* in this study, developing a unique algorithm called `MM-AdaSoC`. Specifically, two submodels in state-space form are generated from a modified Nernst battery model. Both are shown to be locally observable with admissible inputs. The iterated extended Kalman filter (IEKF) is then applied to each submodel in parallel, estimating simultaneously the SoC variable and unknown parameters. The SoC estimates obtained from the two separately implemented IEKFs are fused to yield the final overall SoC estimates, which tend to have higher accuracy than those obtained from a single-model. Its effectiveness is demonstrated using simulation and experiments. The notion of multi-model estimation can be extended promisingly to the development of many other advanced battery management and control strategies.

1. Introduction

Industrial applications of batteries usually require a well-designed management system for operational safety and performance, which monitors the running status and regulates the charging/discharging processes [1]. One of its fundamental functions is to estimate the state-of-charge (SoC), i.e., the percentage ratio of the present battery capacity over its maximum capacity.

1.1. Literature review

SoC estimation has remained an active research field during the past years, and the reader may refer to Ref. [2] for a survey. A notable trend in this area is the increasing emphasis on model-based estimation methods. The dynamic models, derived from either equivalent circuits or electrochemical principles, facilitate the assimilation of the battery data and lead to real-time SoC estimation with bounded errors. While battery modeling has been well-accomplished [3], more attention is being geared towards the development of estimation algorithms. Application of the Kalman filtering (KF) techniques has been remarkable in this respect. The classical linear KF and its extensions to nonlinear systems,

* Corresponding author. Tel.: +1 617 621 7500; fax: +1 617 621 7550.
E-mail address: yebinwang@ieee.org (Y. Wang).

0378-7753/$ – see front matter © 2013 Elsevier B.V. All rights reserved.
http://dx.doi.org/10.1016/j.jpowsour.2013.12.005

including the extended KF (EKF), unscented KF (UKF), iterated extended KF (IEKF), have been used to deal with SoC estimation based on electrochemical and equivalent circuit models, see Refs. [4–13]. A variety of other state observers originating from control theory have also played a role in constructing SoC estimators. Here, we highlight the sliding mode observer [14], adaptive model reference observer [15], Lyapunov-based observer [16] and PDE-based observer [17,18].

Since a good model is a prerequisite, model-based SoC estimation typically is after the procedures of dynamic modeling and parameter identification. However, accurate identification is challenging. First, the parameters in a battery model are often subject to changes with time and operational conditions. For instance, the internal resistance will rise and the capacity diminishes as a result of battery aging. Another example is the charging and discharging efficiencies, which are dependent on the SoC, magnitude of current and temperature. Second, the parameters may differ from one battery to another, making identification for each battery rather cumbersome. Therefore, adaptive approaches are more desirable, merging both identification and SoC estimation in one step. As shown in Fig. 1, an adaptive SoC estimator gives not only the SoC estimates but also the estimates of the model parameters in real time after assimilating the current–voltage data on the basis of a model. The parameter estimates will then be used to update the model to aid the next-step estimation.

Adaptive SoC estimation has been attracting considerable attention in the recent literature. An adaptive EKF-based SoC estimator is designed in Ref. [9], which interacts with a parameter estimator. In Ref. [11], state augmentation is conducted to incorporate the SoC variable and model parameters, and then the UKF is applied to estimate the augmented state. However, the convergence, and as a result, the accuracy, are noted to be difficult to guarantee. In Ref. [13], an adaptive SoC estimator is developed using the IEKF, guided by an analysis of the observability/identifiability. Novel adaptive PDE observers for SoC estimation have also been reported in Ref. [19]. It should be noted that all these existing approaches are based on a single battery model, and here we instead propose to exploit multiple models for better estimation performance.

1.2. Statement of contributions

In this paper, we aim to achieve *adaptive, high-fidelity and easy-to-implement SoC estimation*. For this purpose, we seamlessly link the notion of 'multiple models' and adaptive SoC estimation. A multitude of models, compared to a single one, can give a better description of complicated uncertain dynamics [20–22], thus particularly suitable to deal with the tasks relevant to batteries. The design of the adaptive SoC estimator partially builds on our previous work [13]. In that work, we propose an adaptive approach for SoC estimation via IEKF-based simultaneous state and parameter estimation. While credible estimation is observed, the accuracy is still limited in Ref. [13] by the mismatch between the model and the true system. This fact motivates the development of the `MM-AdaSoC` algorithm in this paper.

An overview of the construction of `MM-AdaSoC` is as follows. First, multiple submodels are brought up from a modified Nernst battery model by fixing some parameters and assuming the others unknown. Each submodel is shown locally observable with admissible inputs by rigorous analysis. Then, an adaptive SoC estimation scheme will be implemented simultaneously but separately to each submodel, with the submodel in each implementation assumed true. The SoC estimates resulting from different submodels will be fused in the light of a certain strategy to obtain the final estimate. As such, we boost the accuracy of SoC estimation despite the presence of uncertainties plaguing battery models.

The main contributions of this paper lie in two aspects. First, this is the first known study of multi-model adaptive SoC estimation to the best of our knowledge, and it is shown that the proposed `MM-AdaSoC` algorithm provides more accurate estimation while maintaining a good balance over the computational cost. Second, we introduce the multi-model framework for battery management and control. In addition to the proposed `MM-AdaSoC`, we discuss various other ways to enhance SoC estimation using multiple models. Many existing battery management strategies can also be improved on a multi-model basis.

1.3. Organization

The rest of the paper is organized follows. Section 2 presents a basic review of the multi-model estimation theory. Section 3 describes the model construction and gives observability analysis. Section 4 combines adaptive SoC estimation and multi-model estimation to establish the `MM-AdaSoC` algorithm, the effectiveness of which is validated in Section 5 by simulation and experimental results. Finally, Section 6 gathers our conclusions and ideas for future work.

2. Basics of multi-model estimation

The structure of a typical multi-model estimator is shown in Fig. 2. In this section, we give a review of the multi-model estimation, with an emphasis on the estimate fusion strategy.

Its first part is composed of a bank of parallel filters based on different models. Each filter assimilates the data to produce its own estimate. All the estimates will then be fused to give the best estimate. Many options exist for the elemental filter, such as the KF for a linear model or the EKF for a nonlinear one. What is of particular interest here is the design of the fusion strategy.

Let us consider a general system. Its unknown state at time instant k is denoted by $\mathbf{x}_k \in \mathbb{R}^{n_x}$ and its measurement by $\mathbf{z}_k \in \mathbb{R}^{n_z}$. Different models are available to describe the system, leading to a model set $\mathbb{M} = \{\mathscr{M}_1, \mathscr{M}_2, \cdots, \mathscr{M}_N\}$. Suppose that $\mathscr{M}_i$ is given by

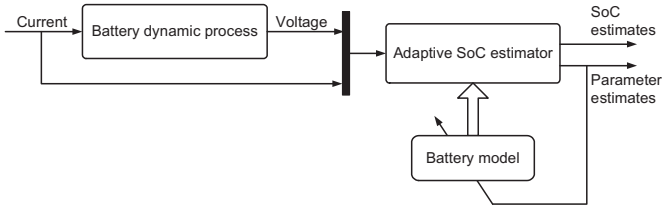

Fig. 1. A schematic description of adaptive SoC estimation.

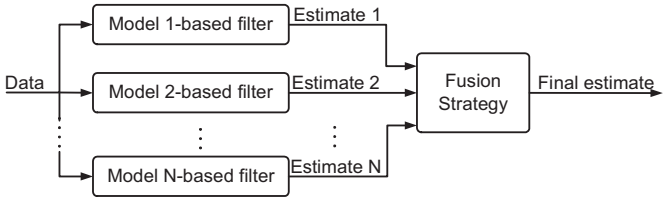

Fig. 2. The structure of a multi-model estimator.

$$\mathscr{M}_i : \begin{cases} \mathbf{x}_{k+1} &= \mathbf{f}^i(\mathbf{x}_k) + \mathbf{w}_k^i, \\ \mathbf{z}_k &= \mathbf{h}^i(\mathbf{x}_k) + \mathbf{v}_k^i, \end{cases} \tag{1}$$

where $\mathbf{f}^i$ and $\mathbf{h}^i$ are C^1 functions to represent the state transition and measurement, respectively, and $\{\mathbf{w}_k^i\}$ and $\{\mathbf{v}_k^i\}$ are uncorrelated, zero-mean, white Gaussian noise sequences with covariances $\mathbf{Q}_k^i \geq 0$ and $\mathbf{R}_k^i > 0$, respectively. While assuming that the true system coincides with one model at each time instant, we do not know which model matches the system at any time. Thus a probabilistic description is used. Let s_k denote the system running status at k. It may take any $\mathscr{M}_i$ for $i = 1, 2, \ldots, N$ to address the uncertainty of model matching. The probability of the event $s_k = \mathscr{M}_i$ is denoted as $p(s_k = \mathscr{M}_i)$, or simply, $p(s_k^i)$. In other words, $p(s_k^i)$ indicates the *a priori* probability that the true model is $\mathscr{M}_i$ at time k. Obviously, $\sum_{i=1}^N p(s_k^i) = 1$.

From a statistical perspective, $\mathbf{x}_k$ and $\mathbf{z}_k$ are continuous random variables and s_k a discrete one. Without causing confusion, we use the symbol p to denote the probability density function (pdf), probability mass function (pmf) or mixed pdf–pmf in the sequel for convenience. We define the information set as $\mathbb{Z}_k = \{\mathbf{z}_1, \mathbf{z}_2, \ldots, \mathbf{z}_k\}$ and intend to estimate $\mathbf{x}_k$ from $\mathbb{Z}_k$, hence considering $p(\mathbf{x}_k|\mathbb{Z}_k)$. By the Bayes' theorem, we have

$$\begin{aligned} p(\mathbf{x}_k|\mathbb{Z}_k) &= \sum_{i=1}^N p\left(\mathbf{x}_k, s_k^i \middle| \mathbb{Z}_k\right) \\ &= \sum_{i=1}^N p\left(\mathbf{x}_k|s_k^i, \mathbb{Z}_k\right) p\left(s_k^i \middle| \mathbb{Z}_k\right). \end{aligned} \tag{2}$$

When $p(\mathbf{x}_k|\mathbb{Z}_k)$ becomes available, we can carry out minimum-mean-square-error (MMSE) estimation or Maximum a Posteriori (MAP) estimation of $\mathbf{x}_k$:

$$\begin{aligned} \text{MMSE} &: \widehat{\mathbf{x}}_{k|k} = \mathrm{E}(\mathbf{x}_k|\mathbb{Z}_k) = \int \mathbf{x}_{k|k} p(\mathbf{x}_k|\mathbb{Z}_k) \mathrm{d}\mathbf{x}_k, \\ \text{MAP} &: \widehat{\mathbf{x}}_{k|k} = \arg\max_{\mathbf{x}_k} p(\mathbf{x}_k|\mathbb{Z}_k). \end{aligned}$$

Independent of the method (MMSE or MAP) used, it follows from (2) that

$$\widehat{\mathbf{x}}_{k|k} = \sum_{i=1}^N \widehat{\mathbf{x}}_{k|k}^i p\left(s_k^i \middle| \mathbb{Z}_k\right), \tag{3}$$

where $\widehat{\mathbf{x}}_{k|k}^i$ is the estimate of $\mathbf{x}_k$ based on the model $\mathscr{M}_i$. An observation from this analysis is that $p(s_k^i|\mathbb{Z}_k)$ turns out to be a probabilistic weight coefficient. The associated estimation error covariance is

$$\begin{aligned} \mathbf{P}_{k|k} &= \mathrm{E}\left[\left(\widehat{\mathbf{x}}_k - \mathbf{x}_k\right)\left(\widehat{\mathbf{x}}_k - \mathbf{x}_k\right)^\top \middle| \mathbb{Z}_k\right] \\ &= \int \left(\widehat{\mathbf{x}}_k - \mathbf{x}_k\right)\left(\widehat{\mathbf{x}}_k - \mathbf{x}_k\right)^\top p(\mathbf{x}_k|\mathbb{Z}_k) \mathrm{d}\mathbf{x}_k \\ &= \sum_{i=1}^N \int \left(\widehat{\mathbf{x}}_k - \mathbf{x}_k\right)\left(\widehat{\mathbf{x}}_k - \mathbf{x}_k\right)^\top p\left(\mathbf{x}_k, s_k^i \middle| \mathbb{Z}_k\right) \mathrm{d}\mathbf{x}_k \\ &= \sum_{i=1}^N \int \left(\widehat{\mathbf{x}}_k - \mathbf{x}_k\right)\left(\widehat{\mathbf{x}}_k - \mathbf{x}_k\right)^\top p\left(\mathbf{x}_k|s_k^i, \mathbb{Z}_k\right) \mathrm{d}\mathbf{x}_k p\left(s_k^i \middle| \mathbb{Z}_k\right) \\ &= \sum_{i=1}^N \left[\mathbf{P}_{k|k}^i + \left(\widehat{\mathbf{x}}_k - \widehat{\mathbf{x}}_k^i\right)\left(\widehat{\mathbf{x}}_k - \widehat{\mathbf{x}}_k^i\right)^\top\right] p\left(s_k^i \middle| \mathbb{Z}_k\right). \end{aligned} \tag{4}$$

Let us take a closer look at $p(s_k^i|\mathbb{Z}_k)$. Using the Bayes' theorem again, we see that

$$\begin{aligned} p\left(s_k^i \middle| \mathbb{Z}_k\right) &= \frac{p\left(s_k^i, \mathbb{Z}_k\right)}{p(\mathbb{Z}_k)} = \frac{p\left(\mathbf{z}_k|s_k^i, \mathbb{Z}_{k-1}\right) p\left(s_k^i|\mathbb{Z}_{k-1}\right)}{p(\mathbf{z}_k|\mathbb{Z}_{k-1})} \\ &= \frac{p\left(\mathbf{z}_k|s_k^i, \mathbb{Z}_{k-1}\right) p\left(s_k^i|\mathbb{Z}_{k-1}\right)}{\sum_{j=1}^N p\left(\mathbf{z}_k, s_k^j \middle| \mathbb{Z}_{k-1}\right)} \\ &= \frac{p\left(\mathbf{z}_k|s_k^i, \mathbb{Z}_{k-1}\right) p\left(s_k^i|\mathbb{Z}_{k-1}\right)}{\sum_{j=1}^N p\left(\mathbf{z}_k|s_k^j, \mathbb{Z}_{k-1}\right) p\left(s_k^j \middle| \mathbb{Z}_{k-1}\right)}. \end{aligned} \tag{5}$$

Furthermore, we have

$$\begin{aligned} p\left(\mathbf{z}_k|s_k^i, \mathbb{Z}_{k-1}\right) &= \int p\left(\mathbf{z}_k, \mathbf{x}_k|s_k^i, \mathbb{Z}_{k-1}\right) \mathrm{d}\mathbf{x}_k \\ &= \int p\left(\mathbf{z}_k|\mathbf{x}_k, s_k^i, \mathbb{Z}_{k-1}\right) p\left(\mathbf{x}_k|s_k^i, \mathbb{Z}_{k-1}\right) \mathrm{d}\mathbf{x}_k \\ &= \int p\left(\mathbf{z}_k|\mathbf{x}_k, s_k^i\right) p\left(\mathbf{x}_k|s_k^i, \mathbb{Z}_{k-1}\right) \mathrm{d}\mathbf{x}_k. \end{aligned}$$

Under the mildly simplified assumption that $p(\mathbf{z}_k|\mathbf{x}_k, s_k^i) = \mathscr{N}(\mathbf{h}^i(\mathbf{x}_k), \mathbf{R}_k^i)$ and $p(\mathbf{x}_k|s_k^i, \mathbb{Z}_{k-1}) = \mathscr{N}(\widehat{\mathbf{x}}_{k|k-1}^i, \mathbf{P}_{k|k-1}^i)$, $p(\mathbf{z}_k|s_k^i, \mathbb{Z}_{k-1})$ can be approximated as

$$p\left(\mathbf{z}_k|s_k^i, \mathbb{Z}_{k-1}\right) \approx (2\pi)^{-\frac{n_\mathbf{z}}{2}} |\mathbf{S}_k^i|^{-\frac{1}{2}} \exp\left[-\frac{1}{2}\left(\tilde{\mathbf{z}}_k^i\right)^\top |\mathbf{S}_k^i|^{-1} \tilde{\mathbf{z}}_k^i\right],$$

where

$$\begin{aligned} \tilde{\mathbf{z}}_k^i &= \mathbf{z}_k - \mathbf{h}^i\left(\widehat{\mathbf{x}}_{k|k-1}^i\right), \\ \mathbf{S}_k^i &= \mathbf{H}_k^i \mathbf{P}_{k|k-1}^i (\mathbf{H}_k^i)^\top + \mathbf{R}_k^i, \\ \mathbf{H}_k^i &= \tfrac{\partial \mathbf{h}^i}{\partial \mathbf{x}}\left(\widehat{\mathbf{x}}_{k|k-1}^i\right). \end{aligned}$$

Furthermore,

$$p\left(s_k^i \middle| \mathbb{Z}_{k-1}\right) = \frac{p\left(\mathbb{Z}_{k-1}|s_k^i\right) p\left(s_k^i\right)}{p(\mathbb{Z}_{k-1})} = p\left(s_k^i\right),$$

since $p(\mathbb{Z}_{k-1}|s_k^i) = 1$ and $p(\mathbb{Z}_{k-1}) = 1$ because $\mathbb{Z}_{k-1}$ is an event with probability 1 at time $k-1$. If we define $\mu_k^i = p(s_k^i|\mathbb{Z}_k)$ and $w_k^i = p(\mathbf{z}_k|s_k^i, \mathbb{Z}_{k-1})$ and suppose $\pi_k^i = p(s_k^i)$, (5) becomes

$$\mu_k^i = \frac{w_k^i \pi_k^i}{\sum_{j=1}^N w_k^j \pi_k^j}. \tag{6}$$

Hence, by (3) and (4), the fusion strategy, or the fuser as is called, is given by

$$\widehat{\mathbf{x}}_{k|k} = \sum_{i=1}^N \widehat{\mathbf{x}}_{k|k}^i \mu_k^i, \tag{7}$$

$$\mathbf{P}_{k|k} = \sum_{i=1}^N \left[\mathbf{P}_{k|k}^i + \left(\widehat{\mathbf{x}}_k - \widehat{\mathbf{x}}_k^i\right)\left(\widehat{\mathbf{x}}_k - \widehat{\mathbf{x}}_k^i\right)^\top\right] \mu_k^i. \tag{8}$$

The final conclusion drawn from this analysis is as follows: the fused estimate (covariance) is a linear weighted combination of the estimates from the elemental filters. It can be noted that

- The estimation is based on a series of elemental filters and the fusion. The process is similar to a ' weight-based reconciliation', which balances the role that different models play in the estimation task.

- The residuals of the elemental filter based on the 'correct' model that best match the true system is expected to be remarkably smaller than those of the others [20]. As a result, the probabilistic weight associated to this filter, say, μ_k^*, will tend to increase and downplay the others. The fused estimate will approach the estimate based on the correct model.

3. Battery models and observability analysis

We investigate the battery modeling in this section. We first develop two submodels from a slightly modified Nernst model and then analyze the local observability properties for each one.

3.1. Construction of multiple battery models

A battery model consists of a set of equations that relate the input (charging/discharging current), the state variables (e.g., SoC) and the output (terminal voltage). Various models have been proposed and used, depending on the specific purposes. For SoC estimation, we consider the Nernst model here [5]:

$$y_k = K_1 + K_2\ln(\mathrm{SoC}_k) + K_3\ln(1-\mathrm{SoC}_k) - Ru_k, \tag{9}$$

where y_k is the terminal voltage at time instant k, u_k is the applied current ($u>0$ for discharging and $u<0$ for charging), R is the internal resistance, and K_i for $i=1, 2, 3$ are constants. To make (9) more capable of grasping the dynamics of certain batteries, we propose the following modification:

$$y_k = K_1 + K_2\ln(\tau_1 + \mathrm{SoC}_k) + K_3\ln(\tau_2 + 1 - \mathrm{SoC}_k) - Ru_k, \tag{10}$$

where two additional constants τ_1 and τ_2 are added. In above, $K_1 + K_2\ln(\tau_1 + \mathrm{SoC}_k) + K_3\ln(\tau_2 + 1 - \mathrm{SoC}_k)$ in (10) can be regarded as the open-circuit voltage (OCV) term. The dynamic change of the SoC is described by the integration of the current over time. In the discrete time, it is given by

$$\mathrm{SoC}_k = \mathrm{SoC}_0 - \sum_{i=0}^{k-1}\frac{\eta\cdot\Delta T}{C_0}u_i,$$

where η is the Coulombic efficiency, C_0 the nominal capacity in ampere-hour (Ah), and ΔT is the sampling period. An equivalent difference equation is

$$\mathrm{SoC}_{k+1} = \mathrm{SoC}_k - K_0u_k, \tag{11}$$

where $K_0 = \eta\cdot\Delta T/C_0$. We then obtain a state-space model for batteries by putting together (10) and (11). The model state is SoC_k and the parameters are K_i for $i=0,\ldots,3$ and R.

For adaptive SoC estimation, we will perform simultaneous estimation of the SoC and the parameters. To obtain a locally observable model, one or several parameters usually need to be fixed in order to estimate the others and the SoC. A few options may exist regarding which parameters are fixed. Based on our experience with the considered model, we separate the parameters into two sets, fix one set and augment the state vector to incorporate the SoC and the other set. Accordingly, two submodels will be constructed.

Letting K_0 and K_1 be fixed, the first one can be obtained:

$$\mathscr{M}_1:\begin{cases}\mathbf{x}_{k+1}^1 &= \mathbf{f}^1(\mathbf{x}_k^1, u_k),\\ y_k &= h^1(\mathbf{x}_k^1, u_k),\end{cases} \tag{12}$$

where

$$\mathbf{x}_k^1 = [\mathrm{SoC}_k\ K_2\ K_3\ R]^\top,$$
$$\mathbf{f}_1(\mathbf{x}_k^1, u_k) = \mathbf{x}_k^1 - [K_0\ 0\ 0\ 0]^\top u_k,$$
$$h_1(\mathbf{x}_k^1, u_k) = K_1 + \mathbf{x}_{k,2}^1\ln(\tau_1 + \mathbf{x}_{k,1}^1) + \mathbf{x}_{k,3}^1\ln(\tau_2 + 1 - \mathbf{x}_{k,1}^1) - \mathbf{x}_{k,4}^1u_k.$$

Analogously, by fixing K_i for $i=1, 2, 3$, we have

$$\mathscr{M}_2:\begin{cases}\mathbf{x}_{k+1}^2 &= \mathbf{f}^2(\mathbf{x}_k^2, u_k),\\ y_k &= h^2(\mathbf{x}_k^2, u_k),\end{cases} \tag{13}$$

where

$$\mathbf{x}_k^2 = [\mathrm{SoC}_k\ K_0\ R]^\top,$$
$$\mathbf{f}^2(\mathbf{x}_k^2, u_k) = [\mathbf{x}_{k,1}^2 - \mathbf{x}_{k,2}^2u_k\ \ \mathbf{x}_{k,2}^2\ \ \mathbf{x}_{k,3}^2]^\top,$$
$$h^2(\mathbf{x}_k^2, u_k) = K_1 + K_2\ln(\tau_1 + \mathbf{x}_{k,1}^2) + K_3\ln(\tau_2 + 1 - \mathbf{x}_{k,1}^2) - \mathbf{x}_{k,3}^2u_k.$$

Remark 1. In an implicit manner, $\mathscr{M}_1$ places more confidence on the state equation (11), assuming that K_0 is accurate, and the belief in the measurement equation (10) is emphasized in $\mathscr{M}_2$ similarly. Nevertheless, it is noteworthy that the confidence level on each submodel during the estimation process is dynamically determined by the fusion strategy outlined earlier in Section 2.

Remark 2. An extended series can be constructed on the basis of each submodel if we let the parameters take different values that are believed to be close or equal to the truth. For instance, the Coulombic efficiency may be 100%, 90% or even 80% depending on the operating conditions. Then $\mathscr{M}_1$ will give birth to three more submodels if K_0 assumes $\Delta T/C_0$, $0.9\Delta T/C_0$ and $0.8\Delta T/C_0$, respectively. This allows considerable flexibility for us to describe the battery dynamics and brings improvements to the single-model case.

3.2. Observability analysis

It is well-known that state estimation requires a 'certain' kind of observability of the system. Hence, we will analyze the observability properties of $\mathscr{M}_1$ and $\mathscr{M}_2$ before proceeding to SoC estimation.

Consider a general single-input-single-output (SISO) system

$$\mathscr{J}:\begin{cases}\mathbf{x}_{k+1} &= \mathbf{f}(\mathbf{x}_k, u_k),\\ y_k &= h(\mathbf{x}_k, u_k),\end{cases} \tag{14}$$

where $\mathbf{x}\in\mathbb{X}$ of dimension n, $y\in\mathbb{Y}$ and $u\in\mathbb{U}$. We assume that 1) $\mathbb{X}$ and $\mathbb{Y}$ connected, second countable, Hausdorff, differentiable manifolds of class C^q with $q\in\mathbb{N}$, 2) $\mathbb{U}$ is an open interval of $\mathbb{R}$, and 3) $\mathbf{f}:\mathbb{X}\times\mathbb{U}\to\mathbb{X}$ and $h:\mathbb{X}\to\mathbb{Y}$ are of class C^q. For convenience, $\mathbf{f}(\mathbf{x},u)$ is denoted as $\mathbf{f}^u(\mathbf{x})$, and $h(\mathbf{f}(\mathbf{x},u_0),u_1) = h^{u_1}\circ\mathbf{f}^{u_0}(\mathbf{x})$. Following [23,24], the local observability for $\mathscr{J}$ is defined as follows:

Definition 1. Distinguishability

Two states $\mathbf{x}$ *and* $\mathbf{x}^*$ *are said to be indistinguishable, written as* $\mathbf{x}\rightleftarrows\mathbf{x}^*$, *if for each* $l\neq 0$ *and for each input sequence,* $\{u_0,\ldots,u_l\}\in\mathbb{U}^l$, *we have*

$$h^{u_l}\circ\mathbf{f}^{u_{l-1}}\circ\ldots\circ\mathbf{f}^{u_0}(\mathbf{x}) = h^{u_l}\circ\mathbf{f}^{u_{l-1}}\ldots\circ\mathbf{f}^{u_0}(\mathbf{x}^*).$$

Otherwise, they are distinguishable.

Definition 2. Local observability

The system $\mathscr{J}$ *is locally observable if for any state* $\mathbf{x}^o\in\mathbb{X}$, *there exists a neighborhood* $\mathbb{D}$ *of* $\mathbf{x}^o$ *such that,* $\mathbf{x}\rightleftarrows\mathbf{x}^*$ *implies* $\mathbf{x} = \mathbf{x}^*$ *for each* $\mathbf{x},\mathbf{x}^*\in\mathbb{D}$.

By Definitions 1 and 2, local observability means that $\mathbf{x}^o$ can be distinguished from its neighbors given the input sequence $\{u_0, \ldots,$

$u_l\}$ and the output sequence $y_0, \ldots, y_l$. It should be noted that this definition of observability depends not only on the system itself but also on the applied inputs, unlike the uniform observability for any inputs defined in [25]. While one sees various definitions of nonlinear observability in the literature, this does not obstruct our discussion since they are usually about 'different measurements results from different initial states (for admissible inputs)'. The interested reader can refer to the literature on the subject, e.g., [26].

To address the observability condition, the following sets of functions are defined:

$$\begin{aligned}&\Omega_0 = \{h(\cdot)\},\\ &\Omega_l = \left\{h^{u_j}\circ\mathbf{f}^{u_{j-1}}\circ\cdots\circ\mathbf{f}^{u_0}(\cdot) : u_i\in\mathbb{U}\,\forall\, i = 1,\cdots,j \text{ and } 1\le j\le l\right\},\\ &\Omega = \cup_{j\ge 0}\Omega_l.\end{aligned}$$

An observability criterion is presented in the following theorem, please see Ref. [23] for the proof.

Theorem 1. In Ref. [23] *If* $\dim \mathrm{d}\Omega(\mathbf{x}) = n\ \forall \mathbf{x}\in\mathbb{X}$, *then the system* $\mathscr{J}$ *is locally observable.*

Theorem 1 gives a sufficient condition to determine the local observability by relating it to the full dimensionality of the codistribution $\mathrm{d}\Omega$. Now the local observability of $\mathscr{M}_1$ and $\mathscr{M}_2$ can be analyzed using Theorem 1. Let us take $\mathscr{M}_1$ for an example since the analysis for both follows similar lines.

Note that $\mathbf{f}^1$ and h^1 are of class C^∞. Suppose that the initial state is $\mathbf{x}_0^1$ for $\mathscr{M}_1$ and that there are L measurements $\{y_1, \ldots, y_L\}$. By (12), $\mathbf{x}_k^1$ is given by

$$\mathbf{x}_k^1 = \mathbf{x}_0^1 - [K_0 \quad 0 \quad 0 \quad 0]^\top \sum_{i=0}^{k-1} u_i.$$

Hence, we have

$$\begin{aligned}\bar{h}_k^1(\mathbf{x}_0^1) = h^{1u_k}\circ\mathbf{f}^{1u_{k-1}}\circ\cdots\circ\mathbf{f}^{1u_0}(\mathbf{x}_0^1) = K_1\\ +\mathbf{x}_{0,2}^1\ln\left(\tau_1+\mathbf{x}_{0,1}^1-K_0\sum_{i=0}^{k-1}u_i\right)+\mathbf{x}_{0,3}^1\ln\left(\tau_2+1-\mathbf{x}_{0,1}^1+K_0\sum_{i=0}^{k-1}u_i\right)\\ -\mathbf{x}_{0,4}^1 u_k,\end{aligned}$$

where $\bar{h}_k^1\in\Omega$. Define a matrix $\mathbf{J}$ with dimensions $L\times 4$:

$$\mathbf{J} = \left[\frac{\mathrm{d}\bar{h}_1^1}{\mathrm{d}\mathbf{x}_0^1} \quad \cdots \quad \frac{\mathrm{d}\bar{h}_k^1}{\mathrm{d}\mathbf{x}_0^1} \quad \cdots \quad \frac{\mathrm{d}\bar{h}_L^1}{\mathrm{d}\mathbf{x}_0^1}\right]^\top.$$

The elements in the k-th row of $\mathbf{J}$ are

$$\begin{aligned}\mathbf{J}_{k,1} &= \frac{\partial\bar{h}_k^1}{\partial\mathbf{x}_{0,1}^1} = \frac{\mathbf{x}_{0,2}^1}{\tau_1+\mathbf{x}_{0,1}^1-K_0\sum_{i=0}^{k-1}u_i} - \frac{\mathbf{x}_{0,3}^1}{\tau_2+1-\mathbf{x}_{0,1}^1+K_0\sum_{i=0}^{k-1}u_i},\\ \mathbf{J}_{k,2} &= \frac{\partial\bar{h}_k^1}{\partial\mathbf{x}_{0,2}^1} = \ln\left(\tau_1+\mathbf{x}_{0,1}^1-K_0\sum_{i=0}^{k-1}u_i\right),\\ \mathbf{J}_{k,3} &= \frac{\partial\bar{h}_k^1}{\partial\mathbf{x}_{0,3}^1} = \ln\left(\tau_2+1-\mathbf{x}_{0,1}^1+K_0\sum_{i=0}^{k-1}u_i\right),\\ \mathbf{J}_{k,4} &= \frac{\partial\bar{h}_k^1}{\partial\mathbf{x}_{0,4}^1} = -u_k.\end{aligned}$$

By observation, we have the following conclusions:

- The submodel $\mathscr{M}_1$ is locally observable if a suitable input sequence $\{u_k\}$ is applied. By 'suitable', we mean that u_k varies sufficiently in magnitude over time, or in other words, $\{u_k\}$ contains a rich mix of frequency contents. In this case, $\mathbf{J}$ will have full column rank, and as a result, $\dim \mathrm{d}\Omega$ has a dimension of 4, satisfying the condition in Theorem 1. Such a condition imposed on the input is a mild constraint that can be easily satisfied when a battery is in use.
- We can analogously determine that $\mathscr{M}_2$ is also locally observable if a suitable $\{u_k\}$ is used to excite the system.
- Additional submodels other than $\mathscr{M}_1$ and $\mathscr{M}_2$ can be constructed by fixing different parameters. An example is to fix only K_1, which will lead to another locally observable model. However, no matter how many submodels are used, the essence of multi-model adaptive SoC estimation remains the same, as will be seen in Section 4. It is also noteworthy that the resultant submodel will be unobservable if all the parameters are assumed unknown.

4. Multi-model adaptive SoC estimation

In this section, we study multi-model adaptive SoC estimation on the basis of Sections 2 and 3. An IEKF-based elemental filter will be applied to $\mathscr{M}_1$ and $\mathscr{M}_2$, respectively, for adaptive SoC estimation. The overall estimate will be obtained by fusing all the estimates for the elemental filters, leading to the `MM-AdaSoC` algorithm.

4.1. Adaptive SoC estimation

Adaptive SoC estimation can be attained via state estimation, because the state vector of each consists of both the SoC variable and the parameters. Following Ref. [13], we use the IEKF. As an improved version of the EKF, it is capable of giving more accurate state estimates even for highly nonlinear systems by iteratively refining the estimate around the current point at each time instant.

Consider applying the IEKF to the system in (14). At $k-1$, prediction can be made about the next time instant. The formulas are as follows:

$$\hat{\mathbf{x}}_{k|k-1} = \mathbf{f}\left(\hat{\mathbf{x}}_{k-1|k-1}, u_{k-1}\right), \tag{15}$$

$$\mathbf{P}_{k|k-1} = \mathbf{F}_{k-1}\mathbf{P}_{k-1|k-1}\mathbf{F}_{k-1}^\top + \mathbf{Q}, \tag{16}$$

where $\hat{\mathbf{x}}$ is the estimate of $\mathbf{x}$, $\mathbf{P}$ is the error covariance, $\mathbf{Q}\ge 0$ is an adjustable matrix to account for the process noise, and $\mathbf{F}$ is given by

$$\mathbf{F}_{k-1} = \frac{\partial\mathbf{f}}{\partial\mathbf{x}}\left(\hat{\mathbf{x}}_{k-1|k-1}, u_{k-1}\right).$$

When the measurement y_k arrives, $\hat{\mathbf{x}}_{k|k-1}$ can be updated by the new information y_k brings. The procedure is based on iteration. Let ℓ denote the iteration number and $\hat{\mathbf{x}}_{k|.k}^{(\ell)} = \hat{\mathbf{x}}_{k|.k-1}$ for $\ell = 0$. The update formulas are

$$\mathbf{K}_k^{(\ell)} = \mathbf{P}_{k|k-1}\mathbf{H}_k^{(\ell-1)}\left[\mathbf{H}_k^{(\ell-1)}\mathbf{P}_{k|k-1}\mathbf{H}_k^{(\ell-1)\top} + R\right]^{-1}, \tag{17}$$

$$\hat{y}_k^{(\ell)} = h\left(\hat{\mathbf{x}}_{k|k}^{(\ell-1)}, u_k\right), \tag{18}$$

$$\hat{\mathbf{x}}_{k|k}^{(\ell)} = \hat{\mathbf{x}}_{k|k-1} + \mathbf{K}_k^{(\ell)}\left[y_k - \hat{y}_k^{(\ell)} - \mathbf{H}_k^{(\ell-1)}\left(\hat{\mathbf{x}}_{k|k-1} - \hat{\mathbf{x}}_{k|k}^{(\ell-1)}\right)\right], \tag{19}$$

where $R>0$ accounts for the measurement noise and

$$\mathbf{H}_k^{(\ell)} = \frac{\partial h}{\partial\mathbf{x}}\left(\hat{\mathbf{x}}_{k|k}^{(\ell)}, u_k\right).$$

The iteration process stops when ℓ achieves the pre-specified maximum iteration number $\ell_{\max}$ or when the error between two

Table 1
The MM-AdaSoC algorithm: Adaptive SoC estimation using multiple models.

initialize the implementation: $k=0$, $\hat{\mathbf{x}}^i_{0|0}=\mathbf{x}_0$, $\mathbf{P}^i_{0|0}=\delta^i\mathbf{I}$, where $\delta^i\gg 0$, for $i=1,2$
repeat
  $k\leftarrow k+1$
  IEKF based adaptive SoC estimation:
  for $i=1$ to 2 **do**
    import the submodel $\mathscr{M}_i$
    $\mathscr{M}_i$-based prediction (time-update):
    project the state ahead to obtain $\hat{\mathbf{x}}^i_{k|k-1}$

$$\hat{\mathbf{x}}^i_{k|k-1}=\mathbf{f}^i(\hat{\mathbf{x}}^i_{k-1|k-1},u_{k-1})$$

    project the error covariance ahead to obtain $\mathbf{P}^i_{k|k-1}$

$$\mathbf{F}^i_{k-1}=\frac{\partial\mathbf{f}^i}{\partial\mathbf{x}^i}\left(\hat{\mathbf{x}}^i_{k-1|k-1},u_k\right),\quad \mathbf{P}^i_{k|k-1}=\mathbf{F}^i_{k-1}\mathbf{P}^i_{k-1|k-1}\mathbf{F}^{i\top}_{k-1}+\mathbf{Q}^i$$

    $\mathscr{M}_i$-based update (measurement-update):
    initialize the iteration procedure: $\ell=0$, $\hat{\mathbf{x}}^{i(0)}_{k|k}=\hat{\mathbf{x}}^i_{k|k-1}$
    while $\ell<\ell_{\max}$ **do**
      $\ell\leftarrow\ell+1$
      compute the Kalman gain matrix

$$\mathbf{H}^{i(\ell)}_k=\frac{\partial h^i}{\partial\mathbf{x}^i}\left(\hat{\mathbf{x}}^{i(\ell)}_{k|k},u_k\right),\quad \mathbf{K}^{i(\ell)}_k=\mathbf{P}^i_{k|k-1}\mathbf{H}^{i(\ell-1)}_k\left[\mathbf{H}^{i(\ell-1)}_k\mathbf{P}^i_{k|k-1}\mathbf{H}^{i(\ell-1)\top}_k+R^i\right]^{-1}$$

      update the state estimate

$$\hat{\mathbf{x}}^{i(\ell)}_{k|k}=\hat{\mathbf{x}}^i_{k|k-1}+\mathbf{K}^{(\ell)}_k\left[y_k-h^i\left(\hat{\mathbf{x}}^{i(\ell-1)}_{k|k},u_k\right)-\mathbf{H}^{(\ell-1)}_k\left(\hat{\mathbf{x}}^i_{k|k-1}-\hat{\mathbf{x}}^{i(\ell-1)}_{k|k}\right)\right]$$

    end while
    assign $\hat{\mathbf{x}}^i_{k|k}=\hat{\mathbf{x}}^{i(\ell_{\max})}_{k|k}$
    update the error covariance

$$\mathbf{P}_{k|k}=\left[\mathbf{I}-\mathbf{K}^{(\ell_{\max})}_k\mathbf{H}^{(\ell_{\max})}_k\right]\mathbf{P}_{k|k-1}$$

    export $\mathscr{M}_i$-based SoC estimate $\widehat{\mathrm{SoC}}^i_k=\hat{\mathbf{x}}^i_{k|k,1}$
  end for
  Estimation fusion
  determine the probability π^i_k that the battery runs on $\mathscr{M}_i$ for $i=1,2$ with $\sum_{i=1}^2\pi^i_k=1$
  for $i=1$ to 2 **do**
    compute the initial weights

$$\mathbf{H}^i_k=\frac{\partial h^i}{\partial\mathbf{x}^i}\left(\hat{\mathbf{x}}^i_{k|k-1},u_k\right),\quad S^i_k=\mathbf{H}^i_k\mathbf{P}^i_{k|k-1}(\mathbf{H}^i_k)^\top+R^i$$

$$\hat{y}^i_{k|k-1}=h^i(\hat{\mathbf{x}}^i_{k|k-1},u_k),\quad \tilde{y}^i_{k|k-1}=y_k-\hat{y}^i_{k|k-1},\quad w^i_k=(2\pi)^{-\frac{n}{2}}(S^i_k)^{-\frac{1}{2}}\exp\left[-\frac{(\tilde{y}^i_k)^2}{2S^i_k}\right]$$

  end for
  compute the normalized weights

$$\mu^i_k=\frac{w^i_k\pi^i_k}{\sum_{j=1}^N w^j_k\pi^j_k}\ \text{for } i=1,2$$

  fuse the SoC estimates from $\mathscr{M}_1$ and $\mathscr{M}_2$

$$\widehat{\mathrm{SoC}}_k=\sum_{i=1}^2\widehat{\mathrm{SoC}}^i_k\mu_i$$

until SoC estimation task ends

consecutive iterations is less than the pre-selected tolerance level. Then $\hat{\mathbf{x}}_{k|k}=\hat{\mathbf{x}}^{(\ell_{\max})}_{k|k}$, and the associated error covariance is given by $\mathbf{P}_{k|k}=[\mathbf{I}-\mathbf{K}^{(\ell_{\max})}_k\mathbf{H}^{(\ell_{\max})}_k]\mathbf{P}_{k|k-1}$.

Following the above description, the IEKF can be applied as an elemental filter to $\mathscr{M}_1$ and $\mathscr{M}_2$. The resultant state estimates are $\hat{\mathbf{x}}^1_{k|k}$ and $\hat{\mathbf{x}}^2_{k|k}$, respectively. Accordingly, the SoC estimates are denoted as $\widehat{\mathrm{SoC}}^1_k=\hat{\mathbf{x}}^1_{k|k,1}$ and $\widehat{\mathrm{SoC}}^2_k=\hat{\mathbf{x}}^2_{k|k,1}$, respectively.

4.2. MM-AdaSoC: multi-model adaptive SoC estimation

The SoC estimates produced from $\mathscr{M}_1$ and $\mathscr{M}_2$, $\widehat{\mathrm{SoC}}^1_k$ and $\widehat{\mathrm{SoC}}^2_k$, respectively, can be combined weightedly to generate the overall estimate $\widehat{\mathrm{SoC}}_k$. In the light of the fusion strategy in (7) and (8), we have

$$\widehat{\mathrm{SoC}}_k=\sum_{i=1}^2 2\widehat{\mathrm{SoC}}^i_k\mu_i, \tag{20}$$

where the weight coefficient μ_i for $i=1,2$ can be determined using (6).

Putting together the results, we obtain the MM-AdaSoC algorithm, as is summarized in Table 1.

Remark 3. The underlying idea of the proposed MM-AdaSoC algorithm is that the IEKF-based adaptive SoC estimation is carried out for multiple models and then the estimation results are fused to yield the overall SoC estimate. For the MM-AdaSoC, the recursive and real-time implementation cuts down the amount of stored data. Meanwhile, higher estimation accuracy is achieved, because the update procedure relies on iterative searching at each recursion. Another noteworthy advantage is that a good balance is maintained between the estimation performance and the computational complexity,

conceding a generally linear moderate increase of the demanded computing power depending on the number of models used.

Remark 4. The applicability of the proposed MM-AdaSoC algorithm to different types of batteries is quite promising. Due to its parameterized characterization, the Nernst model has been found capable of describing the dynamics of many batteries, e.g., nickel metal hydride (NiMH), $LiMn_2O_4$ and $LiCoO_2$. As a result, the MM-AdaSoC algorithm can be well applied to such batteries for its construction based on the Nernst model.

Remark 5. Not limited to the MM-AdaSoC algorithm at all, the role that multi-model estimation can play is more profound. It can be developed as a framework, within which a variety of advanced estimation methods can be built for battery applications. Here, we identify five potential sources of multiple models:

- a set of submodels established from a battery model by fixing certain parameters for adaptive SoC estimation, as we have done in this paper,
- a set of submodels established from a model by assuming different sets of values for model parameters,
- a set of different models constructed in different ways, such as an equivalent-circuit model and an electrochemical-principles-based model,
- a set of models capturing different characteristics of batteries, e.g., the charging and discharging processes, cycling and aging effects, and
- a multitude of (sub)models combining the above four cases.

The multi-model approach promises three-fold benefits.

- It better apprehends the battery dynamics known to be complex and multi-faceted, thus promoting the accuracy and robustness of SoC estimation.
- It reduces the complexity of estimator design, especially when highly nonlinear battery dynamics are involved, in a 'divide-and-conquer' manner. Simple and elegant solutions will be achieved and theoretical analysis is made easier.
- It can even provide useful model interpretation and comparison in some circumstances.

To fully realize its potential and benefits, multi-model estimation/control for batteries needs to be further studied in the future.

5. Application examples

In this section, we present two examples using simulation and experiment data, respectively, to evaluate the MM-AdaSoC algorithm.

Example 1. This example is based on simulation with a model used in [15] for a NiMH battery system. For simulation purpose, we employ certain minor modification, but the obtained model is still a sufficiently accurate representation of the NiMH battery dynamics in most circumstances. The change of SoC is governed by

$$\mathrm{SoC}_{k+1} = \mathrm{SoC}_k - \frac{\eta\cdot\Delta T}{C_0}u_k - \frac{S_D\left(T_{\mathrm{ref}}\right)\cdot\Delta T}{100},$$

where the third term on the right-hand side represents self-discharge with

$$S_D\left(T_{\mathrm{ref}}\right) = k_0\exp\left(-\frac{E_{A,S}}{R_g T_{\mathrm{ref}}}\right)\mathrm{SoC}.$$

Here, $k_0 = 1.0683\times10^7$ per hour, $E_{A,S}/R_g = 6.789$ K, the current efficiency $\eta = 1$ for discharging and 0.99 for charging near 50% SoC, the nominal capacity $C_0 = 1.25$ Ah, the reference temperature $T = 35\ ^\circ$C (308.15 K), and the sampling period $\Delta T = 1$ s. The initial SoC is assumed to be 50%. The terminal voltage is equal to the OCV plus internal-resistance-induced drop, that is,

$$y_k = V_{oc,k} - \overline{R}u_k.$$

The OCV V_{oc} is given by the following equation with the inclusion of voltage hysteresis:

$$V_{\mathrm{oc}} = U_0 + \frac{R_g T_{\mathrm{ref}}}{n_e F}\ln\left(\frac{\mathrm{SoC}_k - \Pi}{1-\mathrm{SoC}_k}\right) + V_{H,k},$$

where the varying voltage hysteresis V_{H} is characterized by an empirical expression

$$V_{\mathrm{H},k+1} = V_{\mathrm{H},k} - \beta\cdot\eta\cdot\left[V_{\mathrm{H},max} + \mathrm{sign}(u_k)\cdot V_{\mathrm{H},k}\right]\cdot\Delta T\cdot u_k.$$

The resistance $\overline{R}$ is described by

$$\overline{R} = \sum_{j=0}^{n} a_j \mathrm{SoC}^j.$$

The Farady's constant $F = 9.6485\times10^{-4}$ C mol^{-1}, $n_e = 1$, $R_g = 8.314$ J mol^{-1} K^{-1}, $U_0 = 1.37$ V, $\Pi = 0.08$, $\beta = 3\times10^{-5}$ C^{-1}, $V_{\mathrm{H},max} = 0.05$ V. The initial V_{H} is 0.005 V. In addition, $a_0 = 4.1252\times10^{-2}$, $a_1 = 8.9691\times10^{-4}$, $a_2 = 1.6760\times10^{-5}$, $a_3 = -1.4435\times10^{-7}$ and $a_4 = 4.7223\times10^{-10}$.

During the simulation, we do not assume that this model is fully available for SoC estimation. Instead, the modified Nernst model presented in Section 3 will be used for approximate description of the above true model. Let $K_0 = \eta\cdot\Delta T/C_0$, $K_1 = U_0$, $K_2 = K_3 = R_g T_{\mathrm{ref}}/(n_e F)$, $\tau_1 = -\Pi$, $\tau_2 = 0$ and $R = a_0$. The current signal applied as the input to the battery was a pseudo-random binary sequence (PRBS) stretched by 100 times over the time axis. Its magnitude is 1 A. A view of the input current and output voltage during the first 2000 time instants is given in Fig. 3(a). Let the true initial SoC be 55% and the initial SoC estimate be 65%. The initial weights assigned to $\mathscr{M}_1$ *and* $\mathscr{M}_2$ are 0.7 and 0.3, respectively.

In this setting, we face hysteresis, model mismatch and incorrect initial estimate, which together make SoC estimation a tougher challenge. As described in previous sections, we consider two submodels, with the first one assuming known K_0 and K_1 and the second assuming known K_1, K_2 and K_3. When the MM-AdaSoC algorithm is applied, Fig. 3(b) shows the estimation of the SoC over time. We see that both $\mathscr{M}_1$- and $\mathscr{M}_2$-based estimates differ from the actual values with bounded errors. However, it turns out that the overall estimates given by the MM-AdaSoC algorithm become more accurate, demonstrating that the estimation errors can be reduced effectively by fusion of the multi-model estimates. The weights of the two models are compared in Fig. 3(c). Obviously, $\mathscr{M}_2$ weighs much more than $\mathscr{M}_1$ in this case. This is because $\mathscr{M}_1$ is sensitive to the initial SoC estimate, relying on the state equation based on Coulomb counting. Furthermore, we also apply the well-known EKF to the modified Nernst model with known K_i for $i = 0, 1, 2, 3$ for SoC estimation. As shown in Fig. 3(d), the EKF yields unreliable results in this situation in comparison to the MM-AdaSoC algorithm.

Example 2. For the experimental evaluation of the MM-AdaSoC algorithm, data was collected from a $LiMn_2O_4$/hard-carbon battery in the Advanced Technology R&D Center, Mitsubishi Electric Corporation. The experiment was conducted using a rechargeable battery test equipment produced by Fujitsu Telecom Networks. The current input was a PRBS signal stretched by 10 times over the time axis with a magnitude of 5 A. Despite many other options, we chose

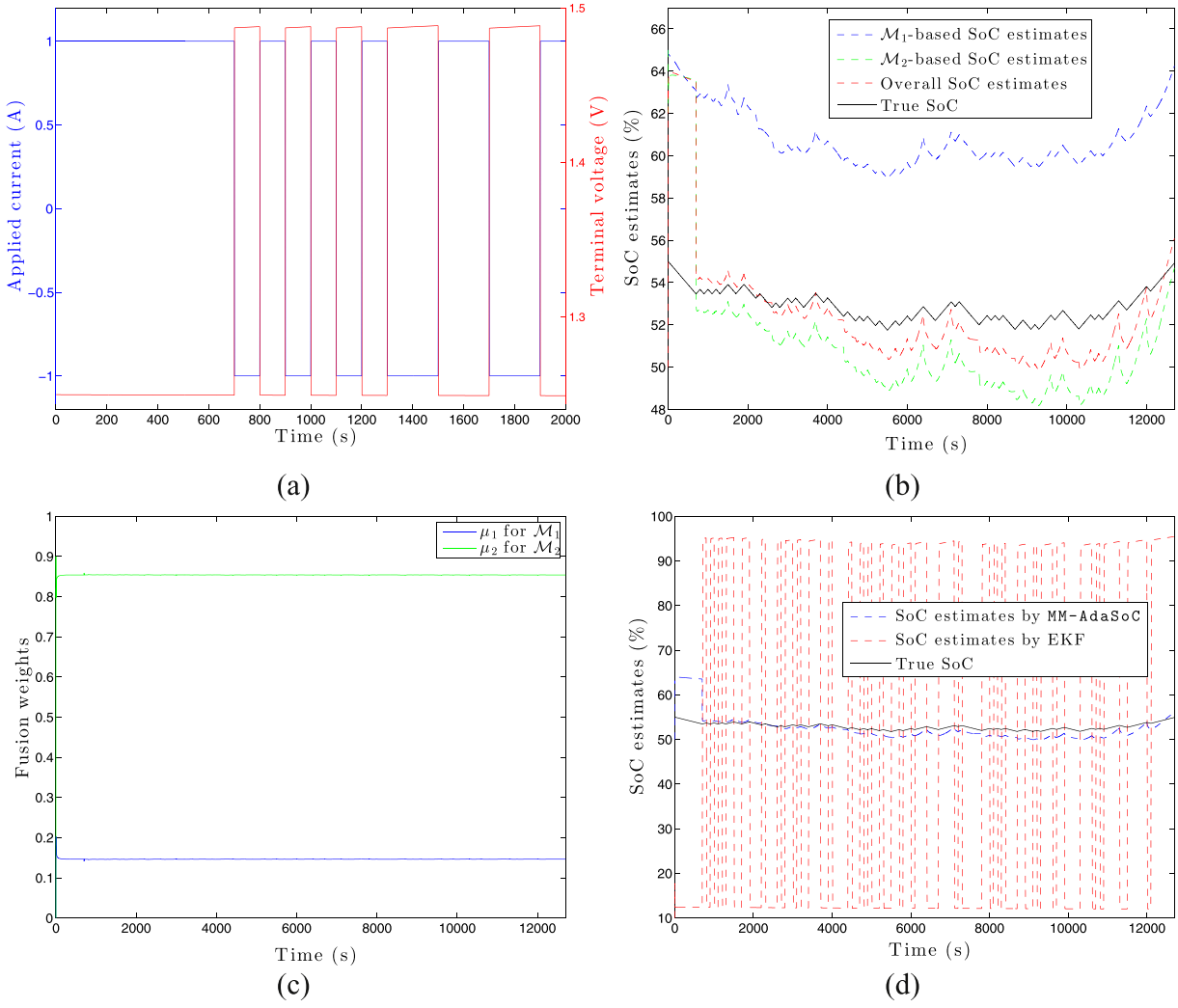

Fig. 3. (a) The input current-output voltage profile; (b) SoC estimates versus truth over time; (c) fusion weights for $\mathcal{M}_1$ and $\mathcal{M}_2$ versus time; (d) comparison with the EKF.

the PRBS because it has white-noise-like properties and is admissible for observability. The profile of the input current and the output voltage is shown in Fig. 4. The battery has a nominal capacity of 4.93 Ah. The sampling period was 1 s. During the experiment, the ambient temperature in the chamber was maintained at 25.8 °C.

We consider the model in (10) and (11). The Coulombic efficiency constant $K_0 = 5.6342 \times 10^{-5}$ when $u_k > 0$ (100% for discharging) and $K_0 = 4.7891 \times 10^{-5}$ when $u_k < 0$ (85% for charging). From the SoC-OCV data collected from this type of batteries, it can be determined that $K_1 = 1.294$, $K_2 = 0.0984$, $K_3 = 3.972$, $\tau_1 = \tau_2 = 0.3$.

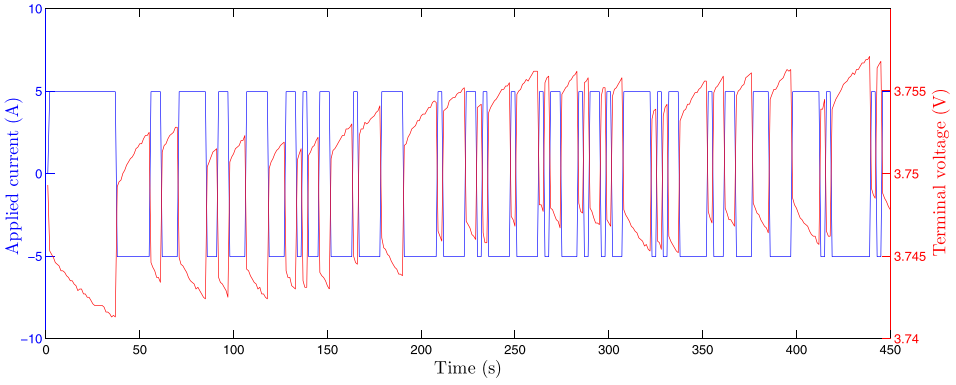

Fig. 4. The input–output (current–voltage) profile.

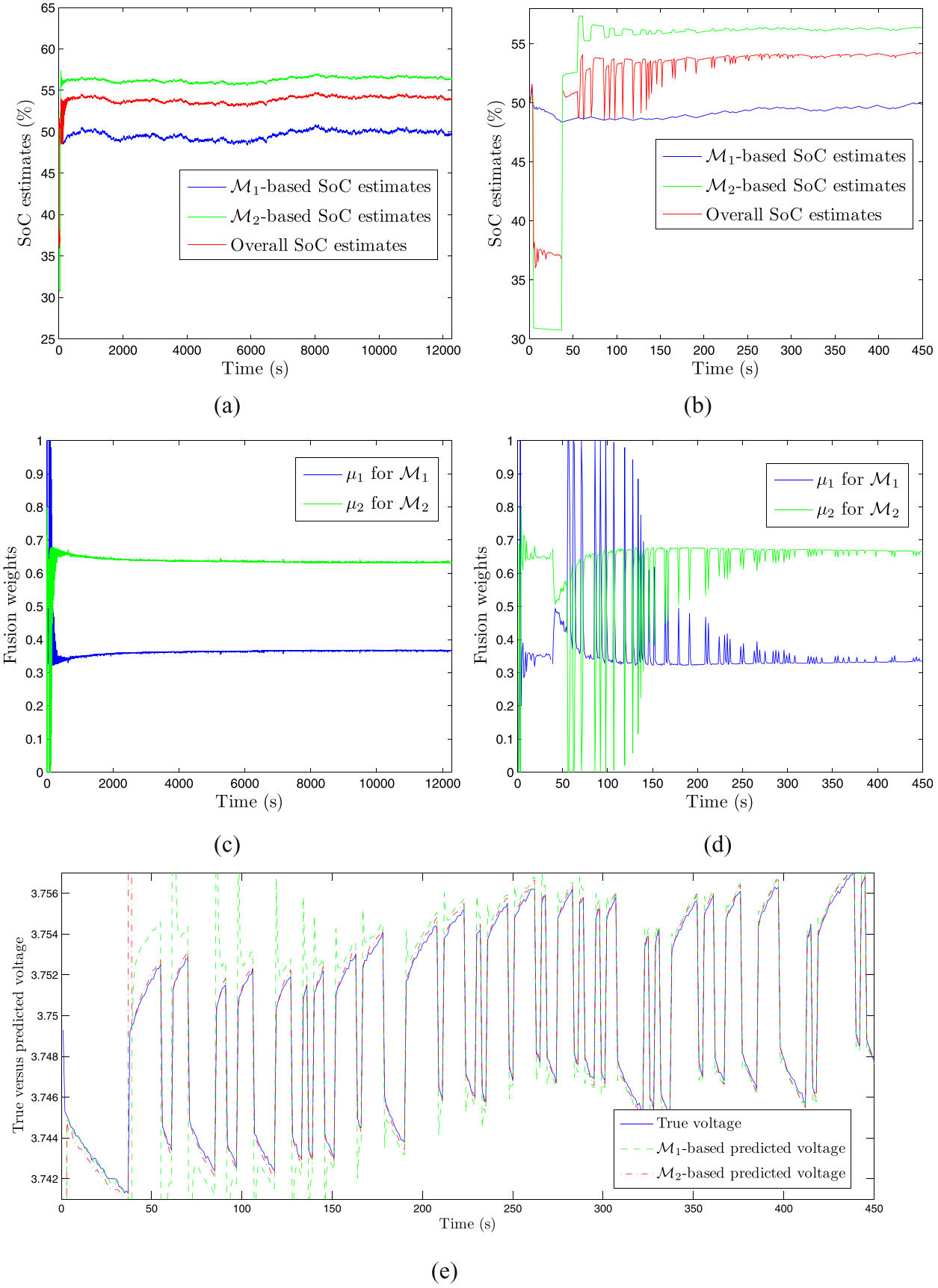

Fig. 5. (a) SoC estimates versus time; (b) SoC estimates during the initial 450 s; (c) fusion weights for $\mathcal{M}_1$ and $\mathcal{M}_2$ versus time; (d) fusion weights during the initial 450 s; (e) comparison between the true and the one-step-forward predicted voltage.

As aforementioned, the actual values of the parameters K_i for $i = 0, \ldots, 3$ can change as a result of the operating conditions. Hence, rather than depending fully on their nominal values, we perform multi-model adaptive SoC estimation by applying the MM-AdaSoC algorithm. The construction of two submodels from (10) and (11) is described in Section 3.1.

The SoC estimation results are shown in Fig. 5. The full view over the available experimental data is given in Fig. 5(a). The initial SoC of the battery is known to be approximately 50%. It is seen that there is a difference of approximately 5% between the $\mathscr{M}_1$-based and $\mathscr{M}_2$-based estimates. Based on our experience, $\mathscr{M}_1$ tends to yield conservative estimates in this case and $\mathscr{M}_2$ does the opposite. The MM-AdaSoC algorithm, through the fusion strategy, makes adjustment to give neutralized overall estimates. Although the true SoC data are not available, we still judge that the estimates are close to the truth, based on our *a priori* knowledge about the battery behavior. Fig. 5(b) illustrates what happens during the initial 450 s. It is seen from Fig. 5(a) and (b) that the overall estimates are closer to those based on $\mathscr{M}_2$. This is verified in Fig. 5(c) and (d), where the weight μ_1 for $\mathscr{M}_1$ fluctuates slightly around 0.63 and μ_2 around 0.37. Thus, with a larger weight, $\mathscr{M}_1$ is given more confidence than $\mathscr{M}_2$ by the MM-AdaSoC algorithm during the implementation. It is understood that the fusion depends on the performance of one-step-forward prediction of the terminal voltage. Fig. 5(e) compares the measured data with the prediction based on $\mathscr{M}_1$ and $\mathscr{M}_2$, respectively. The prediction is satisfactory for both submodels, but $\mathscr{M}_2$ is observed to lead to the better predicted voltage.

From the above results, we believe that the MM-AdaSoC algorithm is quite effective, supported by the findings that the obtained SoC estimates exhibit considerable accuracy and that the voltage prediction approximates the truth well. Through experiments with charging/discharging rates of 0.5 A, 1 A, 10 A and 15 A, we consistently observe similar estimation results, which shows that the applicability of the model and the power of the MM-AdaSoC algorithm.

6. Conclusions

Development of adaptive approaches for SoC estimation is of practical significance, because battery dynamics are often hard to fully determine and are time-varying. We are focused on improving the adaptive SoC estimation via launching a multi-model strategy in this paper, motivated by the proven success of multi-model estimation in addressing problems involving structural and parameter changes.

The main contribution of this paper is the construction and validation of the MM-AdaSoC algorithm. It is built to estimate a battery's SoC in real time through carrying out simultaneous state and parameter estimation on a set of (sub)models. We first construct two submodels from a general state-space battery model by fixing different parameters, with both shown to be locally observable with admissible inputs. The well-known IEKF is then applied to each submodel to produce the SoC and parameter estimates. The final overall estimates are generated by fusing the submodel-based estimates, and it is shown that the fusion is a linear weighted combination of the estimates. Simulation and experimental results are presented to demonstrate and validate the effectiveness of the algorithm.

Apart from the MM-AdaSoC algorithm, we also emphasize the potential of the multi-model framework for battery applications. The initial success reported in this paper would provide strong incentives for further development of a wide range of methods based on multiple models to better monitor the status and health of a battery.

Acknowledgments

The authors would like to thank Prof. Scott Moura for his valuable and constructive suggestions that led to the improvement of this paper.

References

[1] N. Chaturvedi, R. Klein, J. Christensen, J. Ahmed, A. Kojic, IEEE Control Syst. Mag. 30 (3) (2010) 49–68.
[2] V. Pop, H.J. Bergveld, P.H.L. Notten, P.P.L. Regtien, Meas. Sci. Technol. 16 (12) (2005) R93–R110.
[3] R. Rao, S. Vrudhula, D. Rakhmatov, Computer 36 (12) (2003) 77–87.
[4] S. Santhanagopalan, R.E. White, J. Power Sources 161 (2) (2006) 1346–1355.
[5] G.L. Plett, J. Power Sources 134 (2) (2004) 277–292.
[6] D. Domenico, G. Di Fiengo, A. Stefanopoulou, in: Proceedings of IEEE International Conference on Control Applications, 2008, pp. 702–707.
[7] J. Lee, O. Nam, B. Cho, J. Power Sources 174 (1) (2007) 9–15.
[8] J. Han, D. Kim, M. Sunwoo, J. Power Sources 188 (2) (2009) 606–612.
[9] O. Barbarisi, F. Vasca, L. Glielmo, Control Eng. Pract. 14 (3) (2006) 267–275.
[10] K. Smith, C. Rahn, C.-Y. Wang, IEEE Trans. Control Syst. Technol.. ISSN: 1063-6536 18 (3) (2010) 654–663.
[11] G.L. Plett, J. Power Sources 161 (2) (2006) 1369–1384.
[12] S. Santhanagopalan, R.E. White, Int. J. Energy Res. 34 (2) (2010) 152–163.
[13] H. Fang, Y. Wang, Z. Sahinoglu, T. Wada, S. Hara, in: Proceedings of American Control Conference, 2013, pp. 3485–3491.
[14] I.-S. Kim, J. Power Sources 163 (1) (2006) 584–590.
[15] M. Verbrugge, E. Tate, J. Power Sources 126 (1–2) (2004) 236–249.
[16] Y. Hu, S. Yurkovich, J. Power Sources 198 (2012) 338–350.
[17] R. Klein, N. Chaturvedi, J. Christensen, J. Ahmed, R. Findeisen, A. Kojic, IEEE Trans. Control Syst. Technol. 21 (2) (2013) 289–301.
[18] S.J. Moura, N.A. Chaturvedi, M. Krstic, in: Proceedings of American Control Conference, 2012, pp. 559–565.
[19] S.J. Moura, N.A. Chaturvedi, M. Krstic, ASME J. Dyn, Syst. Meas. Control 136 (1) (2013), 011015–011015-11.
[20] P.S. Maybeck, Stochastic Models, Estimation, and Control, vol. 2, Academic Press, New York, 1982.
[21] D. Simon, Optimal State Estimation: Kalman, $\mathscr{H}_\infty$, and Nonlinear Approaches, John Wiley & Sons, 2006.
[22] X. Li, V. Jilkov, IEEE Trans. Aerosp. Electron. Syst. 41 (4) (2005) 1255–1321.
[23] F. Albertini, D. D'Alessandro, Math. Control Sig. Syst. 15 (4) (2002) 275–290.
[24] H. Nijmeijer, A. van der Schaft, Nonlinear Dynamical Control Systems, Springer, 1990.
[25] J.-P. Gauthier, H. Hammouri, S. Othman, IEEE Trans. Autom. Control 37 (6) (1992) 875–880.
[26] R. Hermann, A.J. Krener, IEEE Trans. Autom. Control 22 (5) (1977) 728–740.